American Mineralogist, Volume 79, pages 9–14, 1994

The pressure behavior of α cristobalite

R. T. Downs*

Department of Geological Sciences, Virginia Polytechnic Institute and State University, Blacksburg, Virginia 24061, U.S.A.

D. C. Palmer**

Geophysical Laboratory, Carnegie Institution of Washington, 5251 Broad Branch Road NW, Washington, DC 20015, U.S.A.

Abstract

Structural and volume compressibility data for two α cristobalite samples were determined by single-crystal X-ray diffraction methods at pressures up to ~1.6 GPa. As with the other silica polymorphs that have been studied at high pressure, the change of the Si-O-Si angle is correlated with the volume compressibility. The Si-O bond lengths and the O-Si-O angles remain essentially unchanged. The bulk modulus was determined to be 11.5(7) GPa with a pressure derivative of 9(2). Both crystals underwent reversible structural phase transitions in the pressure interval 1.18–1.60 GPa.

Introduction

The SiO_2 polymorph that is stable at room pressure and at temperatures between 1743 K and its melting point near 1900 K is the cubic phase β cristobalite. The structure continues to exist in a metastable state at temperatures between 1743 and ~500 K. Below ~500 K the structure adopts a tetragonal form, α cristobalite, which is also metastable. The temperature behavior of α and β cristobalite has been studied extensively and was reviewed by Hatch and Ghose (1991) and Schmahl et al. (1992).

Recently there has been interest in developing mathematical models that can describe and predict the structural behavior of the silica polymorphs over a range of pressures (Sanders et al., 1984; Lasaga and Gibbs, 1987, 1988; Gibbs et al., 1988; Stixrude and Bukowinski, 1988; Tsuneyuki et al., 1988; Chelikowsky et al., 1990; van Beest et al., 1990; Boisen and Gibbs, 1993). It is important to have experimental volume and structural data collected at high pressure for a comparison and testing of these models. Such data are available for quartz, coesite, and stishovite. Volume compressibility (Tsuchida and Yagi, 1990), elastic constants, and a negative Poisson's ratio (Yeganeh-Haeri et al., 1992) have been determined for cristobalite, but no structure determinations have been reported as a function of pressure. In this paper, volume and structural data are reported at pressures up to 1.6 GPa for single-crystal α cristobalite.

Room-temperature single-crystal structure refinement

The cristobalite crystals used in this study, collected from Ellora Caves, Hyderabad State, India (Van Valkenburg and Buie, 1945), were kindly supplied by Carl Francis of the Harvard Mineralogical Museum (specimen no. 97849). They occur as single and spinel-twinned gem-quality octahedra in vesicles of Deccan basalt, perched on fibers of mordenite in association with paramorphs of quartz after cristobalite. Untwinned crystals were found and distinguished from the quartz paramorphs by the differences in their refractive indices. In a study of the α-β inversion of cristobalite, Peacor (1973) concluded that the crystals from Ellora Caves probably formed in the metastable region, at temperatures below ~500 K.

A single fragment from a crushed octahedron, with approximate dimensions 125 × 100 × 40 μm, was chosen for a single-crystal X-ray study at room temperature and pressure. A number of peaks in the diffraction pattern were scanned to ensure that they were well formed and that no extra peaks ascribable to twinning were present. The crystal was confirmed to have space group symmetry $P4_12_12$ with cell dimensions a = 4.9717(4) and c = 6.9223(3) Å (Table 1). A complete sphere of intensity data, I_{hkl}, was collected to $(\sin\theta)/\lambda = 0.7$ Å^{-1} on a Rigaku AFC-5R diffractometer with monochromatic Mo$K\alpha$ radiation (λ = 0.7093 Å). A total of 1958 I_{hkl} data were collected and corrected for type I isotropic extinction (Becker and Coppens, 1975). No absorption correction was applied because the linear absorption coefficient was so small (μ_L = 8.545 cm^{-1}). An averaging of the symmetry equivalent reflections resulted in a disagreement index on $|F|$ of 0.018. Of the 171 nonequivalent observations, 146 had $I_{hkl} \geq 2\sigma_I$. The structure was refined with anisotropic temperature factors to a weighted residual of 1.0%, using a revised version of RFINE4 (Finger and

* Present address: Geophysical Laboratory, Carnegie Institution of Washington, 5251 Broad Branch Road NW, Washington, DC 20015, U.S.A.

** Present address: Emmanuel College, Cambridge CB2 3AP, England, and Department of Earth Sciences, University of Cambridge, Downing Street, Cambridge CB2 3EQ, England.

0003–004X/94/0102–0009$02.00

TABLE 1. Cell parameters for cristobalite as a function of pressure

P (GPa)	a (Å)	c (Å)	V (Å³)
		Crystal 1	
0.0	4.9717(4)	6.9223(3)	171.10(1)*
0.19(3)	4.9501(6)	6.8760(6)	168.48(4)*
0.30(3)	4.9304(8)	6.8343(8)	166.13(5)
0.73(3)	4.9028(8)	6.7782(9)	162.93(6)*
1.05(4)	4.8757(8)	6.7163(8)	159.66(6)*
1.30(3)	4.8662(8)	6.6979(7)	158.61(5)
1.50(4)	4.8535(8)	6.6733(8)	157.20(5)
1.60(4)	4.834(6)	6.642(2)	155.2(4)**
		Crystal 2	
0.0	4.975(1)	6.9259(8)	171.42(9)
0.08(3)	4.9662(8)	6.9087(9)	170.39(5)
0.15(9)	4.9608(9)	6.900(1)	169.81(6)
0.15(8)	4.9568(9)	6.890(1)	169.28(6)
0.25(8)	4.9482(9)	6.873(1)	168.27(6)
0.35(8)	4.9404(8)	6.8557(9)	167.33(6)
0.77(8)	4.898(1)	6.768(1)	162.37(6)
0.81(8)	4.902(1)	6.774(1)	162.78(7)
0.29(6)	4.9384(8)	6.8567(9)	167.22(5)
0.30(7)	4.939(1)	6.859(1)	167.31(6)
0.31(6)	4.940(1)	6.854(1)	167.26(7)
0.55(6)	4.917(1)	6.808(1)	164.60(6)
0.52(3)	4.9136(9)	6.8019(9)	164.22(6)
1.06(4)	4.875(1)	6.725(1)	159.82(7)
1.26(3)	4.870(1)	6.709(1)	159.12(7)**
0.09(4)	4.9620(8)	6.8951(9)	169.77(6)
0.79(2)	4.895(1)	6.760(1)	161.98(7)
1.18(3)	4.865(7)	6.724(7)	159.1(4)**

Note: the data are presented in the order in which they were collected. The pressure was adjusted up and down several times for crystal 2.

* Intensity data were collected for these experiments.

** The crystals transformed to a new phase during these experiments.

Prince, 1975). The refined structural parameters and the conditions of refinement are given in Table 2, selected interatomic distances and angles are given in Table 3, and observed and calculated structure factors are listed in Table 4.[1] Additional refinements were undertaken with one and two twin components, according to the twin laws suggested by Dollase (1965). Twin components, if present at all, appear to be <1%.

[1] To obtain a copy of Table 4, order Document AM-94-544 from the Business Office, Mineralogical Society of America, 1130 Seventeenth Street NW, Suite 330, Washington, DC 20036, U.S.A. Please remit $5.00 in advance for the microfiche.

TABLE 2. Intensity collection and refinement results for cristobalite as a function of pressure

P (GPa)	0.0001	0.19	0.73	1.05
No. obs. $I > 2\sigma_I$	146	106	105	102
p*	0.0	0.025	0.04	0.06
Weighted R	0.010	0.040	0.055	0.074
Unweighted R	0.029	0.053	0.056	0.065
u**	0.30028(9)	0.3027(4)	0.3086(4)	0.3125(5)
B(Si)	0.765(7)†	0.80(4)	0.63(5)	0.51(7)
x	0.2392(2)	0.2388(8)	0.2364(10)	0.2356(15)
y	0.1044(2)	0.1086(9)	0.1198(11)	0.1269(15)
z	0.1787(1)	0.1817(5)	0.1870(6)	0.1904(8)
B(O)	1.48(3)†	1.22(9)	1.07(9)	1.12(12)

* Weights were computed by $\sigma = \sqrt{\sigma_I^2 + p^2F^2}$.

** The Si atom is located at Wyckoff position 4a, with coordinates [uu0].

† Values for B(Si) and B(O) at room pressure represent isotropic equivalents of the anisotropic temperature factors given by $\exp\{-\Sigma\Sigma h_i h_k \beta_{jk}\}$, where $\beta_{11} = \beta_{22} = 0.0077(1)$, $\beta_{33} = 0.00401(9)$, $\beta_{12} = -0.0003(2)$, $\beta_{13} = -\beta_{23} = 0.0008(1)$ for Si and $\beta_{11} = 0.0244(7)$, $\beta_{22} = 0.0086(5)$, $\beta_{33} = 0.0062(2)$, $\beta_{12} = -0.0013(4)$, $\beta_{13} = 0.0027(3)$, $\beta_{23} = 0.0005(3)$ for O.

TABLE 3. Selected interatomic distances (Å) and angles (°) for cristobalite as a function of pressure

P (GPa)	0.0001	0.19	0.73	1.05
R(Si-O) × 2	1.603(1)	1.598(5)	1.600(6)	1.602(8)
R(Si-O) × 2	1.603(1)	1.608(4)	1.609(5)	1.610(6)
Si-O-Si	146.49(6)	145.1(2)	142.1(3)	140.4(4)
O-Si-O × 2	108.20(2)	108.2(1)	108.0(1)	107.8(2)
O-Si-O	109.03(9)	109.3(3)	109.6(4)	110.0(5)
O-Si-O × 2	109.99(7)	109.8(3)	109.9(3)	109.8(4)
O-Si-O	111.42(8)	111.6(3)	111.6(4)	111.6(5)

Note: the room-pressure Si-O bond lengths, corrected for rigid body motion (Downs et al., 1992) are 1.611(1) Å.

The structure of a α cristobalite consists of a framework of corner-sharing SiO_4 tetrahedra, each with two nonequivalent SiO bond lengths of 1.603 Å, linked together with Si-O-Si angles of 146.49°. Despite equal bond lengths, the SiO_4 tetrahedra are more distorted than those in either quartz or coesite, two other well-ordered structure types of silica. The O-Si-O angles of the tetrahedra vary between 108.2 and 111.4°, with a tetrahedral angle variance of 1.56°, compared with 0.2 and 0.8° for quartz and coesite. Since all Si-O bonds are equal in length, it is not apparent why the O-Si-O angles depart from cos $-1/3$, given the correlations generally found between the fractional s character of tetrahedral oxyanions, $f_s(T)$, and bond length (Boisen and Gibbs, 1987; Boisen et al., 1990). Selected interatomic angles and bond lengths (Table 3) are in reasonable agreement with the values reported by Dollase (1965), Peacor (1973), and Pluth et al. (1985).

The thermal parameters obtained for the Si and O atoms in all the single-crystal structural studies of α cristobalite, including this one, are large compared with those for quartz or coesite. This has been a matter of concern in previous investigations (Nieuwenkamp, 1937; Dollase, 1965; Peacor, 1973) because large temperature factors are often a sensitive indicator of a twinned or disordered structure, or they can result from significant parameter correlations in the refinement.

In our study, the largest parameter correlation (0.46) was between the scale factor and β_{11} for the Si atom. As the remaining correlations are significantly smaller than 0.46, it appears that problems with correlation are minimal. An examination of the orientations of the thermal ellipsoids shows that the major axis of the O atom is normal to the Si-O-Si plane to within 5°, consistent with Peacor's (1973) observation. Furthermore, the differences in the mean-square displacements of the Si and O atoms along the Si-O bonds and between the intratetrahedral O atoms are small enough to indicate that the SiO_4 tetrahedra behave essentially as rigid bodies (Downs et al., 1990), and therefore the thermal parameters do not contain a significant component of static disorder. Finally, a plot of the average amplitudes of the root-mean square displacements, $\langle u_O^2 \rangle^{1/2}$, recorded for the O atoms in cris-

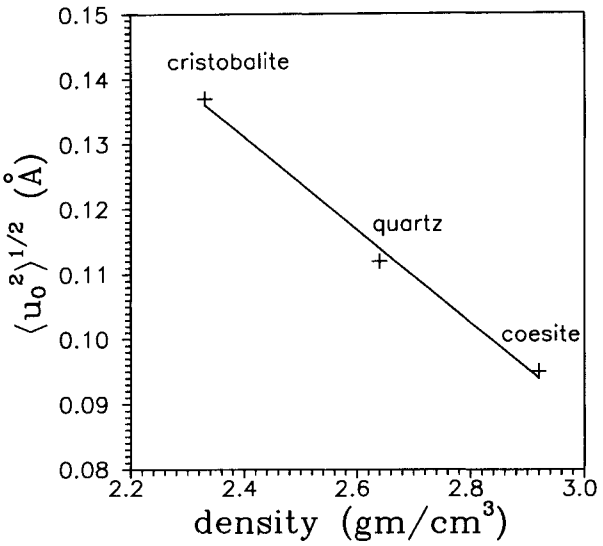

Fig. 1 This plot demonstrates that the average amplitudes of the root-mean square displacements of O, $\langle u_O^2 \rangle^{1/2}$, are negatively correlated with the density of cristobalite, quartz (Kihara, 1990), and coesite (Geisinger et al., 1987). A similar relation holds for the Si atoms, since the ratio of the displacements of O and Si are relatively constant for the silica polymorphs.

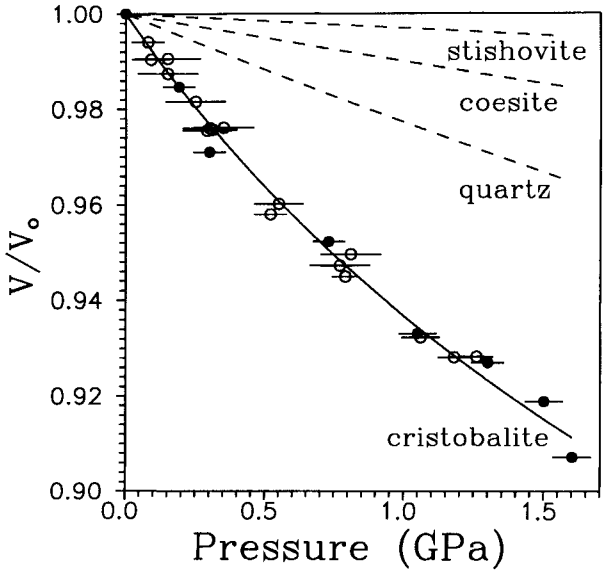

Fig. 2. The unit-cell volume of α cristobalite as a function of pressure. The solid and open circles represent data from crystal 1 and crystal 2, respectively, with the errors in pressure being indicated. The best fit Birch-Murnaghan equation of state [K_0 = 11.5(7) GPa, K_0' = 9(2)] is represented as the solid curve. For comparison, the pressure-volume curves for quartz, coesite, and stishovite are presented as dashed lines. This plot indicates that cristobalite is the most compressible of these SiO_2 polymorphs.

tobalite, quartz, and coesite, shows that $\langle u_O^2 \rangle^{1/2}$ is negatively correlated with density (Fig. 1). It follows that, although the shapes and orientations of the thermal ellipsoids are consistent with relatively large Si-O stretching and O-Si-O angle bending force constants and a relatively small SiO_4 librational force constant, the size of the thermal ellipsoids seems to depend, in part, on the packing density of the tetrahedra.

High-pressure cell refinements

The crystal for which room-pressure data were recorded was transferred to a miniature diamond-anvil cell (modified after Merrill and Bassett, 1974) with a 4:1 methanol to ethanol mixture used as a pressure medium. The crystallographic cell dimensions at each pressure were refined from reflections in the range $30° \leq 2\theta \leq 52°$ that were recorded with the eight-reflection centering technique (King and Finger, 1979) on an automated Picker four-circle diffractometer using Mo$K\alpha$ radiation. The pressure was determined by fitting Lorentzian functions to the fluorescence spectra of several small ruby chips included in the diamond-anvil cell. From the least-squares estimates of the ruby R_1 and R_2 peak positions, the pressure of the experiment was determined using the relationship established by Mao et al. (1978). With this technique, the pressure was determined with a precision better than 0.1 GPa. Diffraction data were recorded at seven pressures up to 1.60(4) GPa, where the crystal transformed into a new, higher pressure structure type, a transformation that was first reported by Yeganeh-Haeri et al. (1990) as occurring around 1 GPa. A least-squares refinement of these data gave the cell dimensions in Table 1. The transformation occurred during data collection, several hours after the pressure of 1.60 GPa was obtained, and took ~20 min to complete, which was calculated based on the rate of diminution of the intensities being collected. Unfortunately, the crystal was lost when it was transferred to the Rigaku diffractometer for a study of its peak shapes.

A second crystal was selected, and diffraction data were recorded at 18 pressures according to the sequence given in Table 1. During this sequence of experiments, the pressure was adjusted up and down several times. At 1.26(3) GPa, the crystal transformed to the high-pressure phase, but it transformed back to α cristobalite when the pressure was lowered. When the pressure was increased once again, the crystal transformed to the high-pressure structure type, but at a slightly lower pressure [1.18(3) GPa]. As with the first crystal, cell dimensions were refined with the data recorded at the pressures indicated in Table 1. The structure of the high-pressure phase is currently being studied, and its Raman spectra are being characterized (Palmer and Finger, 1994).

The unweighted volume, V/V_0, and pressure data recorded for the two crystals (Table 1) were fitted to a third-order Birch-Murnaghan equation of state following the strategies outlined in Bass et al. (1981). The fit yields a zero pressure bulk modulus, K_0 = 11.5(7) GPa, with its pressure derivative, K_0' = 9(2). The volume compressibility curve obtained in the analysis is displayed in Figure 2, along with the data recorded for the two crystals.

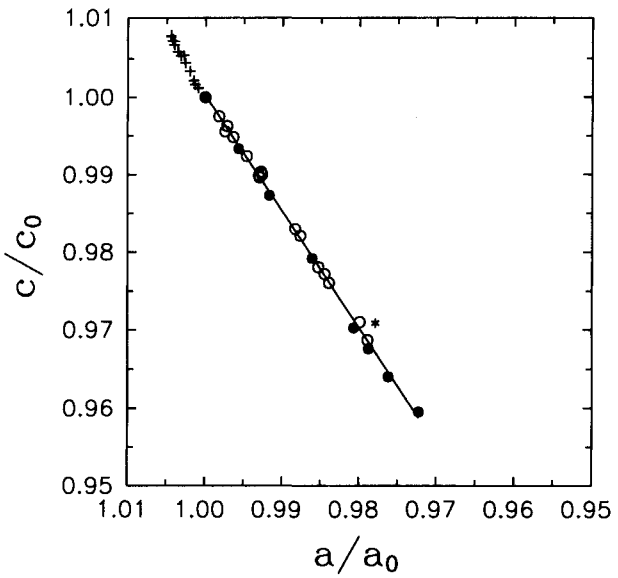

Fig. 3. The variation of c/c_0 vs. a/a_0 for α cristobalite with data recorded at high temperature (+) (Schmahl et al., 1992) and high pressure (solid circles for crystal 1 and open circles for crystal 2). The asterisk represents the last data point for crystal 2 in Table 1 where the crystal underwent a phase transition during the data collection and may be considered an outlier. This plot shows that the relative effects of compression on a/a_0 and c/c_0 remain constant over the pressure interval, with c/c_0 being 1.50(1) times more compressible than a/a_0. Furthermore, the similarity in the slopes of the compression and thermal expansion data appear to indicate that the mechanism for cell-edge variations at high temperature or at high pressure are the same.

The bulk modulus obtained in our analysis is smaller than that determined in a recent Brillouin spectroscopic study (16.4 GPa: Yeganeh-Haeri et al., 1992) and that reported by Tsuchida and Yagi (1990) (18 GPa) obtained through an X-ray diffraction study of a powdered sample without using a hydrostatic medium in their high-pressure cell. This latter study indicated that cristobalite transformed to a new structure at a pressure >10 GPa, somewhat less than that predicted by the molecular dynamics calculation of Tsuneyuki et al. (1989) (16.5 GPa). It appears that the transformation pressure obtained by Tsuchida and Yagi (1990) defined a transition to a phase different from the one reported here.

Figure 2 shows that α cristobalite is much more compressible than either α quartz (K_0 = 41.4 GPa, K_0' = 4: Glinnemann et al., 1992), coesite (K_0 = 95.4 GPa, K_0' = 8.6: Levien and Prewitt, 1981), or stishovite (K_0 = 312.2 GPa, K_0' = 1.8: Ross et al., 1990). The K_0' values obtained for these crystals range from 1.8 for stishovite to 9.0 for cristobalite, with very high uncertainties and no apparent trends.

Figure 3 shows that c/c_0 compresses 1.50(1) times more than a/a_0. Data recorded for α cristobalite at high temperatures (Schmahl et al., 1992) are also plotted for comparison, and it appears that the trend for these data more or less parallels that at high pressure. This could indicate that the compression and expansion mechanisms are the same for cristobalite. It will be shown later that these results are consistent with tilting of the SiO_4 tetrahedra and concomitant Si-O-Si angle bending.

High-pressure structure refinements

Intensity data from the first crystal were recorded for refinements of the structure up to $(\sin\theta)/\lambda$ = 0.7 Å^{-1} at pressures of 0.19, 0.73 and 1.05 GPa on the automated Picker four-circle diffractometer with Mo$K\alpha$ radiation. A summary of the intensity collection procedures and refinement results is provided in Table 2. In particular, the value of the parameter, p, which is used to calculate the regression weights ($\sigma = \sqrt{\sigma_I^2 + p^2F^2}$), was assigned a value that constrained the calculated errors in the diffracted intensities to be distributed normally through a probability plot analysis, according to the strategies of Abrahams and Keve (1971). All parameters varied smoothly with pressure, except for the isotropic temperature factor of the O atom.

Attempts to refine anisotropic thermal parameters resulted in values of β_{ij} that did not indicate the expected rigid body behavior of the SiO_4 tetrahedra. It was concluded that the anisotropic thermal parameters obtained at high pressure did not provide a meaningful measure of the thermal motion, and so the refinement was completed with an isotropic thermal parameter model. Selected bond lengths and angles are found in Table 3, and observed and calculated structure factors are on deposit in Table 4.

Structural variations with pressure

With increasing pressure, the SiO_4 tetrahedron in α cristobalite undergoes only a slight distortion. The Si-O bond lengths remain statistically unchanged, whereas two of the O-Si-O angles show small deviations from values observed at room pressure. The O-Si-O angle that lies more or less parallel to the **c** axis is found to decrease by 0.4°, whereas the one that lies more or less in the **ab** plane increases by 1°. The O atom shifts along the same vector observed by Peacor (1973) in his high-temperature study, but in the opposite direction. Over the 1.05-GPa pressure range that results in a 4.5° tilt of the SiO_4 group about the twofold axis (⟨110⟩ directions) that passes through the Si atom. Rotations of the SiO_4 tetrahedra about these directions have also been shown to be responsible for the strong diffuse scattering observed by electron diffraction of β cristobalite at high temperatures (Hua et al., 1988).

Concomitant with tilting, the Si-O-Si angle decreases by 6° over the 1.05-GPa pressure range. This is a significantly greater angular change than that observed for either quartz or coesite over the same pressure range. To appreciate the relative angular change for the three polymorphs, the normalized Si-O-Si angle, ϕ = ⟨Si-O-Si⟩/⟨Si-O-Si⟩$_0$, was plotted as a function of pressure (Fig. 4a), where ⟨Si-O-Si⟩ is the average Si-O-Si angle at pressure

and $\langle$Si-O-Si$\rangle_0$ is the average angle at room pressure. The trends of ϕ with pressure for the three polymorphs resemble that between V/V_0 and pressure (Fig. 2). When ϕ is plotted against V/V_0 for all three polymorphs, the data fall along a single trend (Fig. 4b) rather than the three distinct trends displayed in Figures 2 and 4a. The solid line drawn through the data in Figure 4b was calculated for both α quartz and α cristobalite, using the SQLOO covalent energy function of Boisen and Gibbs (1993). This function includes terms for Si-O bond stretching, O-Si-O and Si-O-Si angle bending and non-codimer OO repulsion forces obtained from molecular orbital calculations on silicate fragments. The modeled curves for quartz and cristobalite are virtually identical, therefore they are superimposed in the figure as a single line; they do not represent curves fitted to the data. The fact that ϕ and V/V_0 are linearly correlated is not surprising in light of the correlations presented in Figures 2 and 4a. However, that ϕ vs. V/V_0 data for all three polymorphs fall along a single straight line was unexpected. This result implies that the compressibility of these silica polymorphs is controlled in the same manner, by the bending of the Si-O-Si angles and a consequent shortening of the Si-Si distances only. The SQLOO calculations indicate that the change in energy for a given change in volume is larger for quartz than for cristobalite. This is in agreement with the greater compressibility of cristobalite. However, the calculations also indicate that the contribution to the total energy change ascribed to the Si-O-Si bending terms is the same in both structures. That can explain why the calculated curves for both quartz and cristobalite are superimposed in Figure 4b. Since the theoretical data fall along the same trend as the observed data, it appears that the SQLOO model may provide an explanation of the trend. Although no experimental data are available yet for the SiO_2 glasses, also plotted in Figure 4b is a curve fitted to model calculations of the structure of $^{[4]}SiO_2$ glass (Stixrude and Bukowinski, 1991). The figure shows that for a given change in volume (or density) the Si-O-Si angle in glass is not compressed as much as in the crystalline silica polymorphs. Stixrude and Bukowinski (1991) ascribed this different behavior to the torsional degrees of freedom in SiO_2 glass.

The tilting of rigid polyhedra has been shown to be a common characteristic of many structures at high pressure (Hazen and Finger, 1979; Dove et al., 1993) and can be used to describe their structural changes and phase transitions. This appears to be true for cristobalite as well, where the tilting of the SiO_4 tetrahedra is concomitant with bending of the Si-O-Si angle. With an increase in pressure, both the tilting and Si-O-Si angle bending promote the shortening of the c cell edge. On the other hand, although the bending of the Si-O-Si angle promotes shortening of the a cell edge, the tilting of the SiO_4 tetrahedron opposes it. This observation qualitatively explains why the compression of c/c_0 is greater than that for a/a_0 (Fig. 3) and may also suggest a mechanism for the negative Poisson's ratio observed by Yeganeh-Haeri et al. (1992).

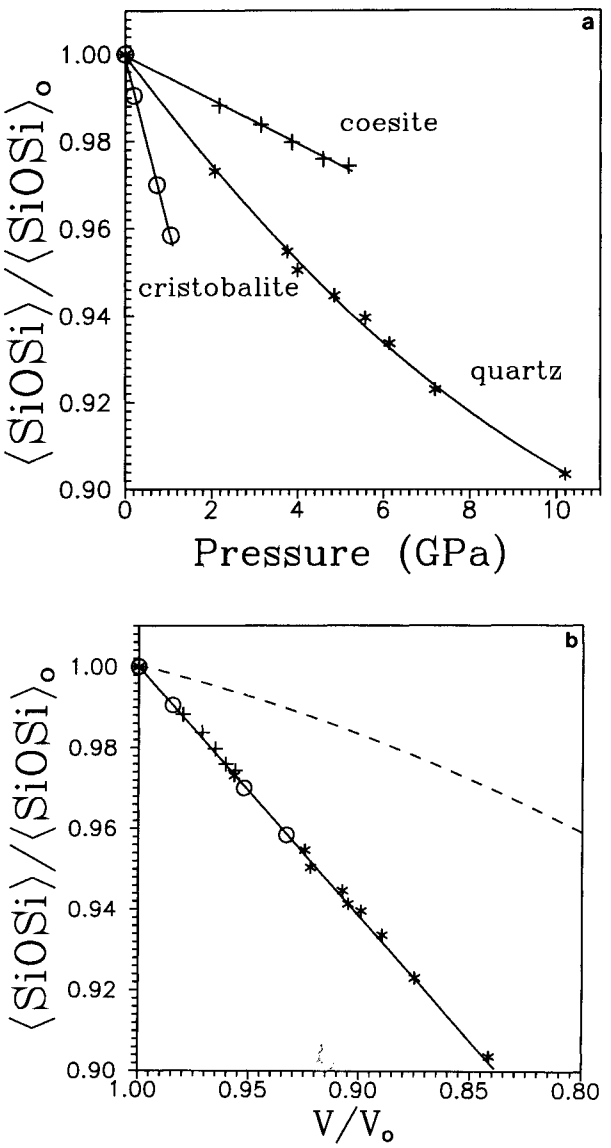

Fig. 4. (**a**) A plot of pressure vs. the normalized average Si-O-Si angles for cristobalite, quartz (Levien et al., 1980; Glinnemann et al., 1992), and coesite (Levien and Prewitt, 1981). The zero-pressure compression rates of the normalized angles are $-0.039(1)$ GPa^{-1} for cristobalite, $-0.0133(4)$ GPa^{-1} for quartz, and $-0.0050(1)$ GPa^{-1} for coesite. This plot indicates that the Si-O-Si angle is most compressible in cristobalite. (**b**) A plot of the normalized unit-cell volume, V/V_0, vs. the normalized average Si-O-Si angle observed for cristobalite, quartz, and coesite. The symbols are the same as in **a**. Superimposed on the plot is a line representing the modeled variations for both cristobalite and quartz. The dashed curve represents a fit to modeled SiO_2 glass (Stixrude and Bukowinski, 1991). A linear regression of the cristobalite, quartz, and coesite data gives $\langle$Si-O-Si$\rangle/\langle$Si-O-Si$\rangle_0 = 0.390(5) + 0.610(5)\ V/V_0$. From this equation we can calculate a Si-O-Si angle of 138.2° at a transition pressure of 1.6 GPa. In surprising contrast to **a**, this plot shows that the normalized Si-O-Si angle varies with volume in the same manner for these crystalline silica polymorphs.

ACKNOWLEDGMENTS

The experimental work reported here could not have been carried out without the kind patronage of Charlie Prewitt, a predoctoral fellowship for R.T.D., and postdoctoral fellowship for D.C.P. Especially acknowledged are the supervision and tutelage of Bob Hazen and Larry Finger. G.V. Gibbs and M.S.T. Bukowinski made major contributions to the manuscript. Ross Angel, M. Mellini, and an anonymous reviewer are thanked for their constructive reviews. The authors would like to thank the National Science Foundation for its generous support through grant EAR-93-03589.

REFERENCES CITED

Abrahams, S.C., and Keve, E.T. (1971) Normal probability plot analysis of error in measured and derived quantities and standard deviations. Acta Crystallographica, A27, 157–165.

Bass, J.D., Liebermann, R.C., Weidner, D.J., and Finch, S.J. (1981) Elastic properties from acoustic and volume compression experiments. Physics of the Earth and Planetary Interiors, 25, 140–158.

Becker, P.J., and Coppens, P. (1975) Extinction within the limit of validity of the Darwin transfer equations. III. Non-spherical crystals and anisotropy of extinction. Acta Crystallographica, A31, 417–425.

Boisen, M.B., Jr., and Gibbs, G.V. (1987) A method for calculating fractional *s*-character for bonds of tetrahedral oxyanions in crystals. Physics and Chemistry of Minerals, 14, 373–376.

——— (1993) A modelling of the structure and compressibility of quartz with a molecular potential and its transferability to cristobalite and coesite. Physics and Chemistry of Minerals, 20, 123–135.

Boisen, M.B., Jr., Gibbs, G.V., Downs, R.T., and D'Arco, P. (1990) The dependence of the SiO bond length on structural parameters in coesite, the silica polymorphs, and the clathrasils. American Mineralogist, 75, 748–754.

Chelikowsky, J.R., King, H.E., Jr., Troullier, N., Martins, J.L., and Glinnemann, J. (1990) Structural properties of α-quartz near the amorphous transition. Physical Review Letters, 65, 3309–3312.

Dollase, W.A. (1965) Reinvestigation of the structure of low cristobalite. Zeitschrift für Kristallographie, 121, 369–377.

Dove, M.T., Giddy, A.P., and Heine, V. (1993) Rigid unit mode model of displacive phase transitions in framework silicates. Transactions of the American Crystallographic Association, 27, 65–75.

Downs, R.T., Gibbs, G.V., and Boisen, M.B., Jr. (1990) A study of the mean-square displacement amplitudes of Si, Al, and O atoms in framework structures: Evidence for rigid bonds, order, twinning, and stacking faults. American Mineralogist, 75, 1253–1267.

Downs, R.T., Gibbs, G.V., Bartelmehs, K.L., and Boisen, M.B., Jr. (1992) Variations of bond lengths and volumes of silicate tetrahedra with temperature. American Mineralogist, 77, 751–757.

Finger, L.W., and Prince, E. (1975) A system of Fortran IV computer programs for crystal structure computations. U.S. National Bureau of Standards, Technical Note, 854, 128 p.

Geisinger, K.L., Spackman, M.A., and Gibbs, G.V. (1987) Exploration of structure, electron density distribution and bonding in coesite with Fourier and pseudoatom refinement methods using single-crystal X-ray diffraction data. Journal of Physical Chemistry, 91, 3237–3244.

Gibbs, G.V., Boisen, M.B., Jr., Downs, R.T., and Lasaga, A.C. (1988) Mathematical modeling of the structures and bulk moduli of TX_2 quartz and cristobalite structure types, T = C, Si, Ge and X = O, S. Materials Research Society Symposium Proceedings, 121, 155–165.

Glinnemann, J., King, H.E., Jr., Schulz, H., Hahn, Th., La Placa, S.J., and Dacol, F. (1992) Crystal structures of the low-temperature quartz-type phases of SiO_2 and GeO_2 at elevated pressure. Zeitschrift für Kristallographie, 198, 177–212.

Hatch, D.M., and Ghose, S. (1991) The α-β phase transition in cristobalite, SiO_2. Physics and Chemistry of Minerals, 17, 554–562.

Hazen, R.M., and Finger, L.W. (1979) Polyhedral tilting: A common type of pure displacive phase transition and its relationship to analcite at high pressure. Phase Transitions, 1, 1–22.

Hua, G.L., Welberry, T.R., Withers, R.L., and Thompson, J.G. (1988) An electron diffraction and lattice-dynamical study of the diffuse scattering in β-cristobalite, SiO_2. Journal of Applied Crystallography, 21, 458–465.

Kihara, K. (1990) An X-ray study of the temperature dependence of the quartz structure. European Journal of Mineralogy, 2, 63–77.

King, H.E., and Finger, L.W. (1979) Diffracted beam crystal centering and its application to high-pressure crystallography. Journal of Applied Crystallography, 12, 374–378.

Lasaga, A.C., and Gibbs, G.V. (1987) Applications of quantum mechanical potential surfaces to mineral physics calculations. Physics and Chemistry of Minerals, 14, 107–117.

——— (1988) Quantum mechanical potential surfaces and calculations on minerals and molecular clusters. I. STO-3G and 6-31G* results. Physics and Chemistry of Minerals, 16, 29–41.

Levien, L., and Prewitt, C.T. (1981) High-pressure crystal structure and compressibility of coesite. American Mineralogist, 66, 324–333.

Levien, L., Prewitt, C.T., and Weidner, D.J. (1980) Structure and elastic properties of quartz at pressure. American Mineralogist, 65, 920–930.

Mao, H.K., Bell, P.M., Shaner, J.W., and Steinberg, D.J. (1978) Specific volume measurements of Cu, Mo, Pd and Ag and calibration of the ruby R_1 fluorescence pressure gauge from 0.06 to 1 Mbar. Journal of Applied Physics, 49, 3276–3283.

Merrill, L., and Bassett, W.A. (1974) Miniature diamond anvil pressure cell for single crystal X-ray diffraction studies. Review of Scientific Instruments, 45, 290–294.

Nieuwenkamp, W. (1937) Über die Struktur von Hoch-Cristobalit. Zeitschrift für Kristallographie, 96, 454–458.

Palmer, D.C., and Finger, L.W. (1994) Pressure-induced phase transition in cristobalite: An X-ray powder diffraction study to 4.4 GPa. American Mineralogist, 79, 1–8.

Peacor, D.R. (1973) High-temperature single-crystal study of the cristobalite inversion. Zeitschrift für Kristallographie, 138, 274–298.

Pluth, J.J., Smith, J.V., and Faber, J., Jr. (1985) Crystal structure of low cristobalite at 10, 293 and 473 K: Variation of framework geometry with temperature. Journal of Applied Physics, 57, 1045–1049.

Ross, N., Shu, J-F., Hazen, R.M., and Gasparik, T. (1990) High-pressure crystal chemistry of stishovite. American Mineralogist, 75, 739–747.

Sanders, M.L., Leslie, M., and Catlow, C.R.A. (1984) Interatomic potentials for SiO_2. Journal of the Chemical Society, Chemical Communications, 19, 1271–1273.

Schmahl, W.W., Swainson, I.P., Dove, M.T., and Graeme-Barber, A. (1992) Landau free energy and order parameter behaviour of the α/β phase transition in cristobalite. Zeitschrift für Kristallographie, 201, 125–145.

Stixrude, L., and Bukowinski, M.S.T. (1988) Simple covalent potential models of tetrahedral SiO_2. Applications to α-quartz and coesite at pressure. Physics and Chemistry of Minerals, 16, 199–206.

——— (1991) Atomic structure of SiO_2 glass and its response to pressure. Physical Review B, 44, 2523–2534.

Tsuchida, Y., and Yagi, T. (1990) New pressure-induced transformations of silica at room temperature. Nature, 347, 267–269.

Tsuneyuki, S., Tsukada, M., Aoki, H., and Matsui, Y. (1988) First-principles interatomic potentials of silica applied to molecular dynamics. Physical Review Letters, 61, 869–872.

Tsuneyuki, S., Matsui, Y., Aoki, H., and Tsukada, M. (1989) New pressure-induced structural transformations in silica obtained by computer simulation. Nature, 339, 209–211.

van Beest, B.W.H., Kramer, G.J., and van Santen, R.A. (1990) Force fields for silicas and aluminophosphates based on *ab initio* calculations. Physical Review Letters, 64, 1955–1958.

Van Valkenburg, A., Jr., and Buie, B.F. (1945) Octahedral cristobalite with quartz paramorphs from Ellora Caves, Hyderabad State, India. American Mineralogist, 30, 526–535.

Yeganeh-Haeri, A., Weidner, D.J., Parise, J., Ko, J., Vaughan, M.T., Liu, X., Zhao, Y., Wang, Y., and Pacalo, R. (1990) A new polymorph of SiO_2 (abs.). Eos, 71, 1671.

Yeganeh-Haeri, A., Weidner, D.J., and Parise, J.B. (1992) Elasticity of α-cristobalite: A silicon dioxide with a negative Poisson's ratio. Science, 257, 650–652.

MANUSCRIPT RECEIVED MARCH 8, 1993
MANUSCRIPT ACCEPTED SEPTEMBER 20, 1993